Biosensors and Bioelectronics 87 (2017) 157–163

Contents lists available at ScienceDirect

Biosensors and Bioelectronics

journal homepage: www.elsevier.com/locate/bios

Dendritic structure DNA for specific metal ion biosensor based on catalytic hairpin assembly and a sensitive synergistic amplification strategy

Jianmin Zhao, Pei Jing, Shuyan Xue, Wenju Xu *

Key Laboratory of Luminescent and Real-Time Analytical Chemistry (Southwest University), Ministry of Education, School of Chemistry and Chemical Engineering, Southwest University, Chongqing, 400715 PR China

ARTICLE INFO

Article history:
Received 12 May 2016
Received in revised form
19 July 2016
Accepted 11 August 2016
Available online 12 August 2016

Keywords:
Electrochemical biosensor
Pb^{2+} detection
Catalyzed hairpin assembly
Dendritic structure DNA
Pb^{2+}-specific DNAzymes

ABSTRACT

In this work, a sensitive electrochemical biosensing to Pb^{2+} was proposed based on the high specificity of DNAzymes to Pb^{2+}. The response signal was efficiently amplified by the catalytic hairpin assembly induced by strand replacement reaction and the formation of dendritic structure DNA (DSDNA) by layer-by-layer assembly. Firstly, in the presence of Pb^{2+}, the substrate strand (S1) of the Pb^{2+}-specific DNAzymes was specifically cleaved by Pb^{2+}. Secondly, one of the two fragments (rS1) introduced into the electrode surface was hybridized with a hairpin DNA (H1) and further replaced by another hairpin DNA (H2) by the hybridization reaction of H1 with H2. The released rS1 then induced the next hybridization with H1. After repeated cycles, the catalytic recycling assembly of H2 with H1 was completed. Thirdly, two bioconjugates of Pt@Pd nanocages (Pt@PdNCs) labeled with DNA S3/S4 and electroactive toluidine blue (Tb) (Tb-S3-Pt@PdNCs and Tb-S4-Pt@PdNCs) were captured onto the resultant electrode surface through the hybridization of S3 and H2, S3 and S4, resulting in the formation of DSDNA triggered by layer-by-layer assembly. This formed DSDNA greatly facilitated the immobilization of manganese(III) *meso*-tetrakis (4-N-methylpyridiniumyl)-porphyrin (MnTMPyP) as mimicking enzyme. Under the synergistic catalysis of Pt@PdNCs and MnTMPyP to H_2O_2 reduction, the effective signal amplification of the developed Pb^{2+} biosensor was achieved. As a result, the sensitive detection of the proposed electrochemical strategy for Pb^{2+} was greatly improved in the range of 0.1 pM–200 nM with a detection limit of 0.033 pM.

1. Introduction

All the time, the sensitive, fast and cost-effective detection of toxic heavy metal ions such as Hg^{2+}, Pb^{2+}, Ag^{+}, and Cr^{3+} at trace or ultra-trace level was focused in environment control (Sobin et al., 2011; Gao et al.; 2016). Up to now, sensitive, rapid and inexpensive sensing system for different metal ions have already been reported, which were involved in electrochemistry (Gao et al., 2012; Zhang et al., 2015a), fluorimetry (Ju et al., 2014; Zhang and Chen, 2014; Gao et al., 2015a) and colorimetry (Huang et al., 2014; Gao et al., 2015b). To some extent, these proposed platforms showed desirable improvement of analytical performance.

As well known, DNAzymes (also called deoxyribozymes), isolated via in vitro selection technique, are capable of performing a specific chemical and biological reactions (Cuenoud et al., 1995; Liu et al., 2009). Interestingly, among them, metal ion-specific DNAzymes possess really high specificity to a particular metal ion. And the metal-binding specificity, binding site, and binding strength can be tuned. In the presence of certain metal ion, its specific DNAzymes could be specifically identified and cleaved at ribonucleotide site (rA). So using of such DNAzymes specific to different metal ions, such as Cu^{2+}, Pb^{2+}, Zn^{2+} and UO_2^{2+}, in different detection systems is very desirable for improving the selectivity and specificity of analytical methods (Carmi et al., 1998; Carmi et al., 2001; Santoro et al., 1997; Li et al., 2000; Liu et al., 2007). Accordingly, 8–17 DNAzyme, a kind of metal ion-specific DNAzymes, is a DNA metalloenzyme catalyzing RNA transesterification in the presence of Pb^{2+} and exhibit high binding specificity to Pb^{2+} through selective cleavage at rA by Pb^{2+}. Meanwhile the activity of DNAzymes is positively correlated to the concentration of Pb^{2+} (Li and Lu, 2000). Therefore, some facile methods based on this reaction have been reported to specifically detect Pb^{2+} (Yin et al., 2009a, 2009b). Meanwhile, the sensitive detection of Pb^{2+} is always of significance. Currently, it has been reported that many electrochemical biosensors for detecting Pb^{2+} were constructed by combining Pb^{2+}-specific DNAzymes with different signal amplification strategies, and

* Corresponding author.
E-mail address: xwju@swu.edu.cn (W. Xu).

http://dx.doi.org/10.1016/j.bios.2016.08.032
0956-5663/

showed high specificity and sensitivity in analytical performance (Li et al., 2013; Tang et al., 2013; Cui et al., 2015).

As well known, catalytic hairpin assembly (CHA), as a kind of nucleic-acid amplification strategies, can be obtained simply by mixing hairpin probes and DNA species without the involvement of exogenous primer and enzyme (Hun et al., 2015; Li et al., 2011). CHA is simpler, lower-cost and more stable over other amplification methods such as polymerase chain reaction (PCR) and rolling circle amplification (RCA) (Yin et al., 2008; Jiang et al., 2013). So, many biosensors for the assay of metal ion, proteins, DNA and microRNA were widely reported by using CHA to amplify response signal (Chen et al., 2013; Liu et al., 2015; Tao et al., 2015; Zhang et al., 2015b; Wu et al., 2016).

More interestingly, dendritic structure DNA (DSDNA) based on layer-by-layer assembly triggered by the hybridization reaction of DNA (Xu et al., 2014; Zhang et al., 2014b), was an efficient immobilizing method for biomolecules and nanomaterials. Owing to the excellent stability (Astruc et al., 2010), DSDNA has received particular attention in developing biosensors based on different analytical methods (Meng et al., 2014). Meanwhile, due to the in situ assembly of DSDNA, nanomaterials or biomolecules with excellent electrocatalytic capacity can be effectively captured, which are very favorable for the response signal amplification. Benefited from this, the efficient improvement of analytical performance of the biosensing platforms for different targets can be successfully achieved. Sun et al. used nanoscale DNA-Au dendrimer as signal amplifier to construct a sensitive surface-enhanced Raman scattering biosensor for Pb^{2+} detection (Sun et al., 2011). While, our research group constructed a sensitive aptasensor for thrombin determination by employing three-dimension DNA-Au@Pt nanoparticles as nanocarriers (Zheng et al., 2016). Besides MnTPP, manganese(III) meso-tetrakis (4-N-methylpyridyl)-porphyrin (MnTMPyP) was also reported to show excellent peroxidases-like activity (Groves., 2000). Importantly, mimicking enzyme MnTMPyP molecules can be efficiently captured into double-strand DNA (dsDNA) scaffold by binding with AT and GC base pairs without requiring specific sequence, which can greatly avoid the limitation of binding amount of MnTMPyP in the labeling process (Pasternack et al., 1983; Nitta et al., 2006). Undoubtedly, MnTMPyP as mimicking enzymes exhibited more desirable catalytic activity in developing electrochemical biosensors (Xie et al., 2014; Liu et al., 2014), compared with traditional enzymes such as horseradish peroxidase or glucose oxidase.

Inspired by the above observations, herein a new electrochemical biosensing strategy for the sensitive detection of Pb^{2+} was proposed based on Pb^{2+}-specific DNAzymes as recognition element, the catalytic hairpin assembly and in situ assembly of DSDNA labeled on Pt@Pd nanocages (Pt@PdNCS), which possessed large surface area and splendid catalytic performance (He et al., 2012). Meanwhile, mimicking enzyme MnTMPyP molecules were embedded into the formed dsDNA scaffold. Under the synergistic catalysis of Pt@PdNCs and MnTMPyP with outstanding catalytic activity to the decomposition of H_2O_2, the electrochemical response signal could be significantly amplified. As a result, coupling with the high specific identification of Pb^{2+}-specific DNAzymes, the effective improvement and the great promotion of sensitivity and specificity, as well as other analytical performances were successfully achieved.

2. Experimental

2.1. Reagents and materials

Hexanethiol (96%, HT), toluidine blue (Tb), palladium potassium chloride (K_2PdCl_4), chloroplatinic acid (H_2PtCl_6), gold chloride ($HAuCl_4$), poly (vinyl pyrrolidone) (PVP, MW ≈55 000), potassium bromide (KBr), L-ascorbic acid (AA) were brought from Sigma (St. Louis, MO, USA). We purchased manganese(III) *meso*-tetrakis (4-*N*-methylpyridyl)-porphyrin (MnTMPyP) from J&K Chemical Technology Co., Ltd. (Beijing, China). Roche (Switzerland) provided Tris (hydroxymethyl) aminomethane hydrochloride (Tris-HCl) for use. The single-strand DNA oligonucleotides were synthesized by Sangon Biotech (Chongqing, China), the sequences of which are listed as followed:

Hairpin DNA H1: 3′-NH_2-$(CH_2)_6$-*CCTTCTCTACTCTGAGTCATCTG-TAGAGAA GG*-5′;.

Hairpin DNA H2: 3′-**TTCCACAAAT***CCTTCTCTACAGATGACTCA-GAGTAGA GAAGG*-5′;.

Pb^{2+}-specific DNAzymes substrate strand (S1): 3′-CTCA-GAGTAGAGAAGGrA TATCACTCA-5′ (the sequence marked with underlined letters refers to rS1);.

Pb^{2+}-specific DNAzymes catalytic strand (S2): 3′-TGAGTGA-TAAAGCTGGCCG AGCCTCTTCTCTAC-5′;.

DNA strand (S3): 3′-NH_2-$(CH_2)_6$-TCTTAACATGA**ATTTGTGGAA**-5′;.

DNA strand (S4): 3′-NH_2-$(CH_2)_6$-**TTCCACAAAT**TGTACAATTCT-5′.

These base sequences marked with italic letters of H1 and H2, underlined letters of H1 and S1, and bold letters of H2, S3 and S4, respectively were complementary each other.

In this work, 0.1 M phosphate-buffered solution (PBS, pH 7.0) was used as working buffer consisted of 0.1 M Na_2HPO_4, 0.1 M KH_2PO_4, 0.1 M KCl. All oligonucleotide solutions for DNA hybridization reaction were prepared by using 10 mM Tris-HCl (pH 7.0) containing 1 M NaCl and 1 mM EDTA. Deionized water (DI water) was used throughout the experiment process.

2.2. Instrumentation

Cyclic voltammetry (CV), differential pulse voltammetry (DPV) and electrochemical impedance spectroscopy (EIS) were carried out with a CHI 660D electrochemical workstation (Shanghai Chenhua Instruments, China), which was equipped with a conventional three-electrode system: a saturated calomel reference electrode as reference electrode, a platinum wire as supporting electrode and a modified glass carbon electrode (GCE) as working electrode. The pH of all used solutions was detected with a pHS-3C meter (MP 230, Mettler-Toledo, Switzerland). The scanning electron micrographs (SEM) of synthesized nanocomposites were tracked by the scanning electron microscopy (S-4800, Hitachi, Tokyo, Japan) at an acceleration voltage of 30 kV and by the thermal field emission scanning electron micrographs (JSM-7800F, JEOL, Japan) at an acceleration voltage of 5 kV.

2.3. Preparation of Pt@Pd nanocages (Pt@PdNCs)

According to the reported method (Zhang et al., 2011), Pt@Pd nanocages (Pt@PdNCs) were prepared. Firstly, 8 mL mixture containing 105 mg PVP, 60 mg AA, 600 mg KBr and KCl was heated to 80 °C under stirring for 10 min, then 3 mL K_2PdCl_4 (57 mg) was added slowly. After kept at 80 °C for 3 h, the product Pd nanocubes (PdNCs) were centrifuged and washed three times using DI water to remove excess PVP, and redispersed in 10 mL DI water. Next, 33.3 mg PVP, 300 mg KBr, and 300 mg AA were dissolved in 7 mL DI water, in which 1 mL PdNCs was added, and the resulting mixture was heated to 90 °C under stirring. After that, 1 mL H_2PtCl_6 (1%, *w/w*) was slowly added at a rate of 1 mL/min, and kept at 90 °C for 12 h. Finally, the obtained Pt@PdNCs were collected by centrifugation and redispersed in 2 mL of DI water for further use.

2.4. Preparation of two bioconjugates of Pt@PdNCs with S3 and S4 (Tb-S3- Pt@PdNCs and Tb-S4-Pt@PdNCs)

100 μL S3 (2.5 μM) or S4 (2.5 μM) added in 1 mL Pt@PdNCs was

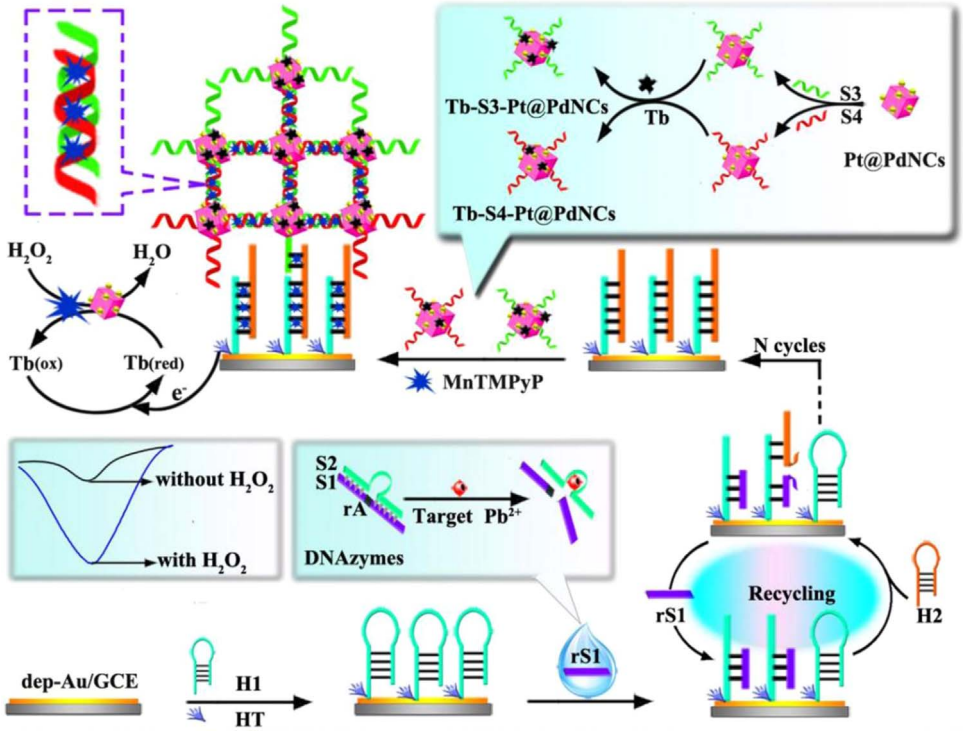

Scheme 1. Schematic illustration of the prepared process of the proposed biosensor for Pb^{2+} detection.

stirred for 10 h at 4 °C. Then 100 μL Tb (0.1 M) was introduced and stirred for another 6 h to form bioconjugates of Tb-S3-Pt@PdNCs or Tb-S4-Pt@PdNCs. Through centrifugation and washing, Tb-S3-Pt@PdNCs or Tb-S4-Pt@PdNCs was obtained and again dispersed in 500 μL DI water. Moreover, two other bioconjugates of PdNCs with S3 and S4 were prepared using the similar method (Tb-S3-PdNCs and Tb-S4-PdNCs). When not use, all of them were stored in refrigerator at 4 °C for next use.

2.5. Fabrication of the proposed biosensor

The specific fabrication process of the proposed biosensor for metal ion was shown in Scheme 1. Firstly, 5 μL S1 (2.5 μM) and 5 μL S2 (2.5 μM) were mixed and heating to 95 °C to form DNAzymes specific to Pb^{2+}. Then 5 μL Pb^{2+} solution with different concentrations was added into the cooled solution. After kept for 0.5 h at 37 °C, the specific cleavage interaction of DNAzymes with Pb^{2+} was completed. Secondly, when clean glass carbon electrode (GCE) was electrodeposited in $HAuCl_4$ solution at −0.2 V potential for 30 s to obtain dep-Au, followed by the incubation of 10 μL NH_2-terminated H1 (2.5 μM) for 16 h and 20 μL HT (1 mM) for 40 min 15 μL of DNAzymes interacted with Pb^{2+} (containing rS1) was introduced into the resulting electrode surface for keeping 1.5 h. After 10 μL H2 (2.5 μM) was incubated to the electrode for another 1.5 h, CHA of H2 induced by the strand replacement was finished. Thirdly, 10 μL Tb-S3-Pt@PdNCs, 10 μL Tb-S4-Pt@PdNCs and 10 μL MnTMPyP were finally dropped onto the obtained electrode surface for 2 h, leading to the formation of DSDNA by the hybridization of S3 and S4 and embedding of MnTMPyP into the formed dsDNA scaffold. Thus, for the proposed biosensor, the electrochemical signal from Tb as the redox probe was dependent on the concentration of target Pb^{2+} in the sample.

3. Results and discussion

3.1. Characterization of PdNCs and Pt@Pd nanocages (Pt@PdNCs)

Fig. 1 showed SEM images of PdNCs and Pt@PdNCs with different resolutions. From Fig. 1A and B, PdNCs displayed cubic morphology and average edge length of each was about 20 nm. When Pt nanoparticles were further developed on PdNCs, the formed Pt@PdNCs exhibited cubic shape and coarse surface, with a slightly larger size than that of original Pd cubes, as shown in Fig. 1C and D. And meanwhile, a darker contrast in the center relative to the edges could be observed, implying a hollow structure in the interior of Pt@PdNCs (Zhang et al., 2011). These suggested successful preparation of PdNCs and Pt@PdNCs, and their micromorphology was comparable to those reported in the publications (Zhang et al., 2011; Xie et al.; 2014).

3.2. Characterization of the proposed biosensor

To demonstrate the modification process of the proposed biosensor, CV response was investigated in $[Fe(CN)_6]^{3-/4-}$ solution (5 mM) at 100 mV/s scan rate, and the result was shown in Fig. 2. Obviously, the bare GCE had a well-defined redox peak in $[Fe(CN)_6]^{3-/4-}$ solution (curve a). The electrodeposition of Au nanoparticles (dep-Au) on bare GCE surface resulted in an increase of the peak current (curve b), indicating that dep-Au with good conductivity promoted the electron transfer. When hairpin DNA H1 and HT as the blocking agent were sequentially incubated into the resultant electrode surface, two significant decreases of the response signal were observed (curve c and curve d), suggesting the great hindrance of nonconductive H1 and HT to the electron transfer. When the prepared Pb^{2+}-specific DNAzymes interacted with 100 nM Pb^{2+} containing rS1 segment was further introduced, the hybridization reaction of rS1 and H1 was triggered,

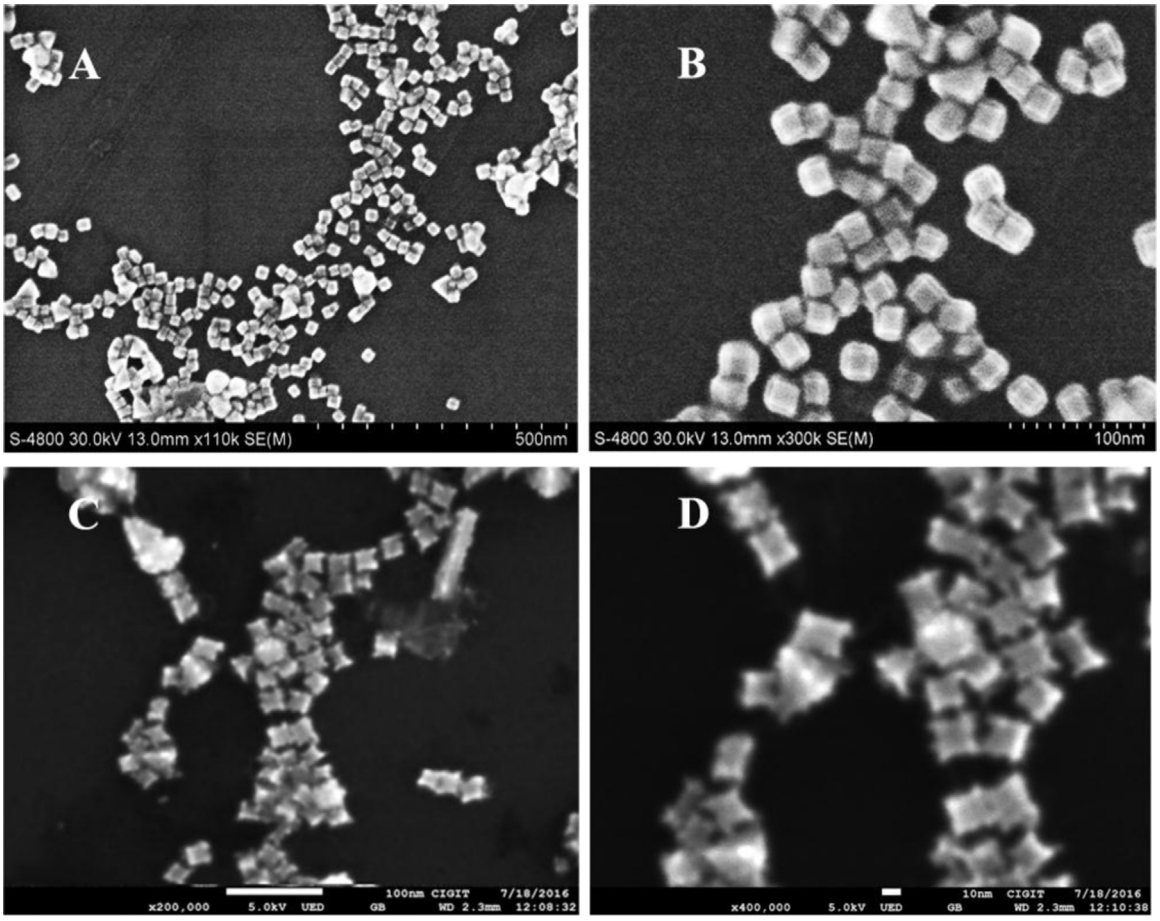

Fig. 1. SEM images of PdNCs (A and B) and Pt@PdNCs (C and D) at different magnifications.

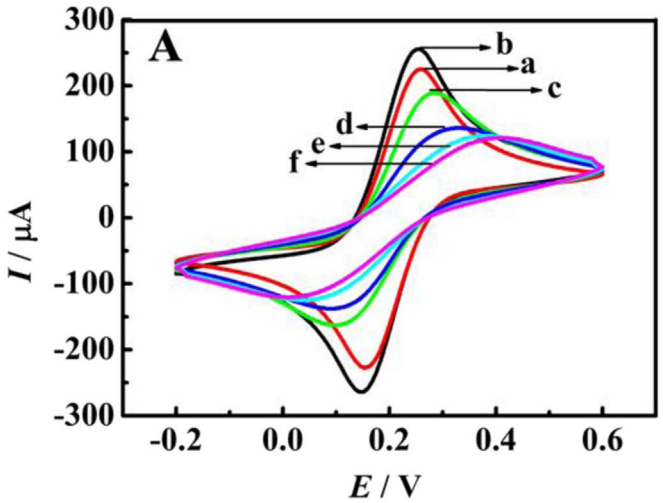

Fig. 2. CVs of different modified electrodes in 1 mL 5 mM $[Fe(CN)_6]^{3-/4-}$ (pH 7.4): (a) bare GCE, (b) dep-Au/GCE, (c) H1/dep-Au/GCE, (d) HT/H1/dep-Au/GCE, (e)rS1/HT/H1/dep-Au/GCE, (f) H2/rS1/HT/H1/dep-Au/GCE.

causing reducing of peak current (curve e). Equally, the subsequent incubation of hairpin DNA H2 also led to further decrease of CV response signal (curve f). This was attributed to that the hybridization between H1 and H2 released rS1 by strand replacement reaction. So the released rS1 continuously induced the catalytic hairpin assembly (CHA) of H2, and complete binding of H2 with H1 after repeated recycles. Meanwhile, the electrochemical impedance spectroscopy (EIS) of the proposed biosensor was also measured in $[Fe(CN)_6]^{3-/4-}$ solution (5 mM) and the results were represented in Fig. S1.

3.3. Comparison of different signal amplification strategies

In this work, Pb^{2+}-specific DNAzymes was used as high specific recognition element to the target Pb^{2+}. Meanwhile, Pt@PdNCs as the nanocarriers were used to immobilize DNA S3 and S4 through Pt-NH_2 bound, and Tb as the redox probe was introduced to form two different bioconjugates of Tb-S3-Pt@PdNCs and Tb-S4-Pt@PdNCs. Along with MnTMPyP, they were captured to the electrode surface modified by CHA of H2, triggering the formation of DSDNA through complementary hybridization reaction between S3 and S4. Meanwhile, MnTMPyP molecules were embedded into dsDNA scaffold. Just because of the self-assembly of DSDNA in the electrode surface, numerous Pt@PdNCs and MnTMPyP were presented in the substrate interface. Thus the decomposition of H_2O_2 was efficiently catalyzed under the synergistic interaction of Pt@PdNCs and MnTMPyP, leading to great promotion of electron transfer of Tb and significant amplification of electrochemical response signal. As a result, the improvement of analytical performance could be achieved for the developed Pb^{2+} biosensor. In order to demonstrate the validity of the proposed amplification strategy, experimental conditions for measuring the electrochemical DPV response were firstly optimized (see supporting information). Under optimal the conditions, DPV signals of different amplifications were also investigated in 0.1 M PBS (pH 7.0) before and after adding 2.22 mM H_2O_2, which were involved in other three incubations in fabricating the biosensors after H2 CHA: (i) Tb-S3-Pt@PdNCs and MnTMPyP in the absence of Tb-S4-Pt@PdNCs, (ii) Tb-S3-Pt@PdNCs

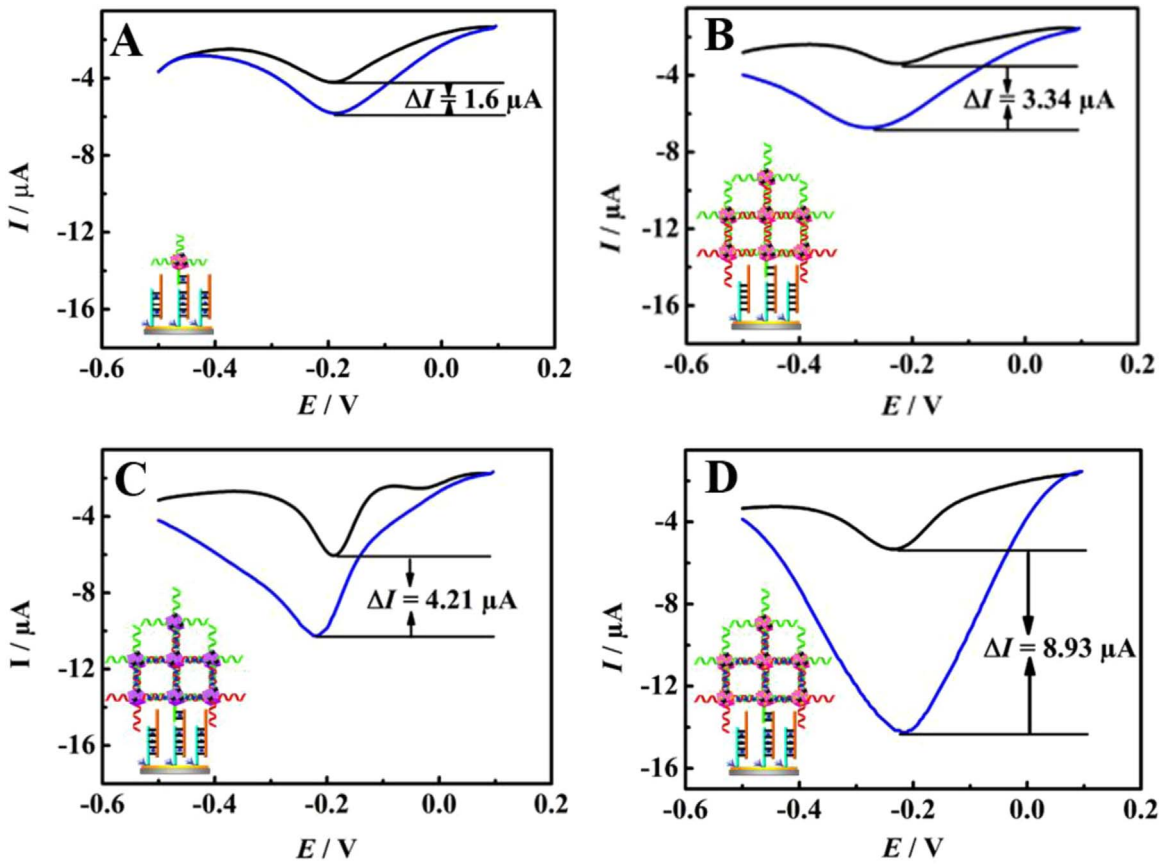

Fig. 3. DPV response of the biosensors in different incubations (A) Tb-S3-Pt@PdNCs and MnTMPyP in the absence of Tb-S4-Pt@PdNCs, (B) Tb-S3-Pt@PdNCs and Tb-S4-Pt@PdNCs in the absence of MnTMPyP, (C) Tb-S3-PdNCs, Tb-S4-PdNCs and MnTMPyP, (D) Tb-S3-Pt@PdNCs, Tb-S4-Pt@PdNCs and MnTMPyP. The tested solution was 0.1 M PBS (pH 7.0) before (black line) and after (blue line) adding 2.22 mM H_2O_2.

and Tb-S4-Pt@PdNCs in the absence of MnTMPyP, (iii) Tb-S3-PdNCs, Tb-S4-PdNCs and MnTMPyP. The results are shown in Fig. 3, in which each change of response signal ($\Delta I = I - I_0$, where I_0 and I are peak current before and after adding 2.22 mM H_2O_2) was listed. From Fig. 3A, B and C, only 3.34 μA, 1.6 μA and 4.21 μA of ΔI were clearly observed for the three cases (i), (ii) and (iii), respectively. However, as can be seen from Fig. 3D, larger increase of ΔI (8.93 μA) was obtained for the proposed amplification strategy. The above experimental observations may be originated from the following three points. (a) Only with Tb-S4-Pt@PdNCs, the self-assembly of DSDNA could be formed by the continuing hybridization reaction of S3 with S4, resulting in the presence of numerous dsDNA in the electrode surface. (b) Compared with PdNCs, Pt@PdNCs with much more surface atoms and loading capacity as nanocarriers (Lim and Xia, 2011) were beneficial for the immobilization of redox probe Tb and showed favorable catalytic activity. (c) Due to DSDNA, mimicking enzyme MnTMPyP molecules with peroxidase-like activity can be enormously embedded into dsDNA scaffold through interacting with AT and GC base pairs (Xu et al., 2013). Therefore, the electrochemical signal could be effectively amplified under the synergetic catalysis of Pt@PdNCs and MnTMPyP to the reduction of H_2O_2, indicating that the improvement of sensitivity and analytical performance of the proposed biosensor could be successfully achieved.

3.4. Analytical performance of the proposed electrochemical biosensor

Based on the high specificity of Pb^{2+}-specific DNAzymes and the self-assemble formation of DSDNA by the trigger of CHA, the improved analytical performance of the proposed biosensor was investigated to different-concentration Pb^{2+} standards under the optimal conditions. The corresponding DPV response measured in 0.1 M PBS (pH 7.0) containing 2.22 mM H_2O_2 was shown in Fig. 4A. Obviously, the response signal in DPV increased with the rising of Pb^{2+} concentration in the range of 0.1 pM to 200 nM, indicating that higher concentration Pb^{2+} in the tested sample gave stronger electrochemical response signal. This may be originated from the fact more Pb^{2+} specifically cleaved more DNAzymes, and more generated rS1 further promoted CHA of more H2 and the formation of DSDNA, which resulted in the presence of numerous redox probe Tb in the electrode surface. Moreover, from Fig. 4B, the peak current showed significant dependence on the logarithm of Pb^{2+} concentration ($\lg c_{Pb^{2+}}$) with a regression equation of $I = -1.393 \lg c_{Pb^{2+}} - 11.83$ and a correlation coefficient of 0.9931. The limit of detection (LOD) was calculated to be 0.033 pM based on the $3s_{blank}$ rule. Compared with other published methods for Pb^{2+} detection, the proposed biosensor exhibited desirable linear range and detection limit shown in Table S1, which benefited from the synergetic biocatalysis of Pt@PdNCs and MnTMPyP based on the effective formation of DSDNA in the sensing electrode interface.

3.5. Specificity, stability and reproducibility study

Under the same conditions, the selectivity of the proposed electrochemical Pb^{2+} biosensor was investigated by using this platform to separately detect other potential interfering metal ions such as Mg^{2+}, Ca^{2+}, Cd^{2+}, Cu^{2+}, Hg^{2+}, Ba^{2+} (each with the same concentration of 10 μM) and their mixture with Pb^{2+} (100 nM). Fig. 5A displayed the DPV response measured in 0.1 M PBS (pH 7.0)

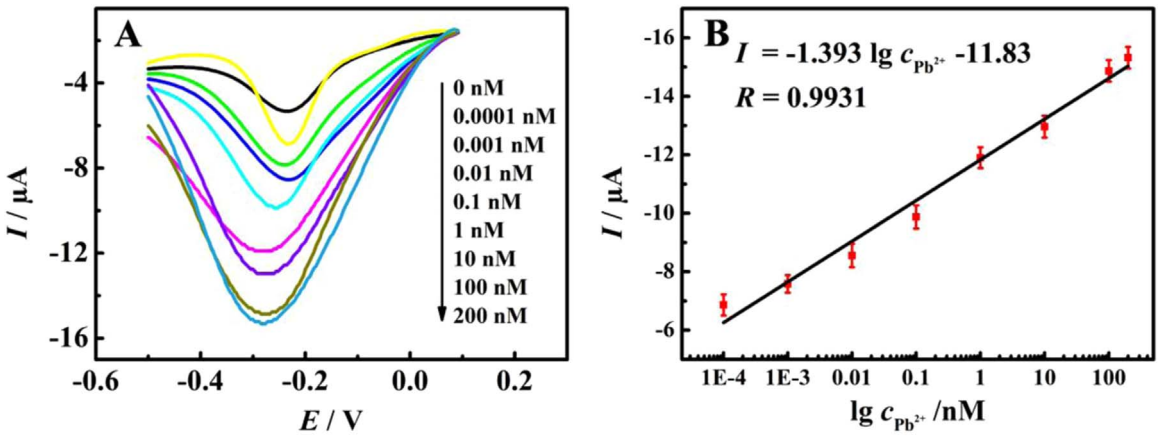

Fig. 4. (A) DPV response of the proposed biosensor to different concentrations of Pb^{2+} in 0.1 M PBS (pH 7.0) containing 2.22 mM H_2O_2. (B) The resulting calibration plot of the peak current vs. $lgc_{Pb}{}^{2+}$ (nM) from 0.1 pM to 200 nM. Error bars: SD, $n=3$.

containing 2.22 mM H_2O_2. As could be seen, the response signal from the tested interferents was almost the same as that of the blank solution. And their mixture with Pb^{2+} gave similar DPV peak current to alone Pb^{2+}, although the concentration of Pb^{2+} was lower 10 times than those of the interfering ions. This indicated the inherent high specificity of the developed platform sensing Pb^{2+}, due to the high specific recognition and cleavage of certain DNAzymes to Pb^{2+}.

When the proposed Pb^{2+} biosensor was stored at 4 °C for 5 and 10 days, the corresponding DPV signal was evaluated in 0.1 M PBS (pH 7.0) with 2.22 mM H_2O_2. From the result shown in Fig. 5B, the response signal still remained 93.2% and 90.7% of its initial value after storing five days and 10 days, respectively, thus implying relative long-term stability of the proposed platform. Under the optimal conditions, five repetitive experiments were carried out in 0.1 M PBS (pH 7.0) with 2.22 mM H_2O_2, and a relative standard deviation (RSD) of 5.6% was obtained, demonstrating that the proposed protocol was coupled with good reproducibility.

3.6. Analysis application of the proposed biosensor in water samples

To demonstrate the applicability of the developed platform in actual samples, standard addition method was used to evaluate Pb^{2+} in tap water obtained from the lab and lake water collected from Congde Lake located in the campus in our university. The water samples were firstly pretreated by centrifuging, and added with different concentrations of Pb^{2+} standard solutions. Then the recovery analysis in the samples was investigated by measuring the DPV response of the proposed sensor in PBS (pH 7.0) containing 2.22 mM H_2O_2. As shown in Table S2, the recovery of Pb^{2+} in two water samples was in the range of 94.7–105% (RSD from 2.6% to 5.0%) and 95.6–107% (RSD from 2.3% to 5.8%). The obtained experimental results further confirmed that the proposed platform sensing Pb^{2+} showed good accuracy and reliability when used to detect Pb^{2+} in real samples, which would be promising and potential for the environmental and biological analysis.

4. Conclusions

In summary, we reported a new electrochemical strategy for specific and sensitive detection of metal ion (Pb^{2+} as the tested model) based on Pb^{2+}-specific DNAzymes as the recognition element. Through the CHA induced by strand replacement reaction and in situ layer-by-layer assembly of DSDNA, numerous Pt@PdNCs with excellent catalytic capacity were captured, accompanying with amount embedding of mimicking enzyme MnTMPyP molecules into the formed dsDNA scaffold. Without the involvement of enzyme, Pt@PdNCs and MnTMPyP cooperatively catalyzed the decomposition of H_2O_2, leading to the efficient amplification of electrochemical response signal and significant improvement of analytical performance for the developed biosensor. The proposed approach coupled the high specificity of Pb^{2+}-specific DNAzymes with the greatly synergistic catalysis of

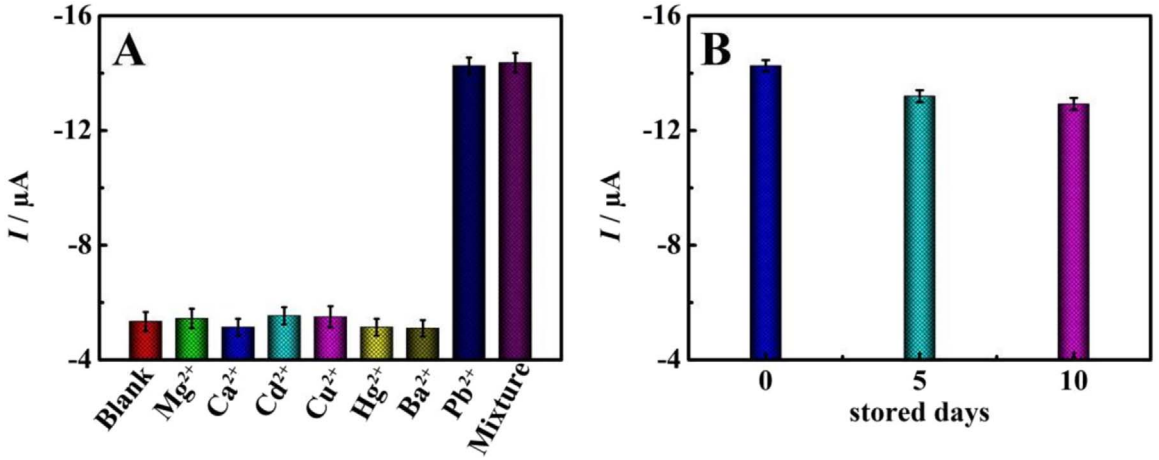

Fig. 5. (A) Selectivity investigations against Mg^{2+}, Ca^{2+}, Cd^{2+}, Cu^{2+}, Hg^{2+}, Ba^{2+} with the same concentration of 10 μM and their mixture with 100 nM Pb^{2+}. (B) Stability of the proposed biosensor after storing 0, 5 and 10 days, respectively. DPV response was measured in 0.1 M PBS (pH 7.0) with 2.22 mM H_2O_2. Error bars, SD, $n=3$.

nanomaterials Pt@PdNCs and mimicking enzyme MnTMPyP assisted by DSDNA and CHA, which resulted in the successful achievement for highly specific and sensitive detection of target Pb^{2+}. The preliminary application of the developed electrochemical platform in actual samples showed good reliability with high accuracy. This would make the proposed strategy hold great potential for selective and sensitive determination of a wide range of target analytes, as long as changing the corresponding specific DNAzymes.

Acknowledgments

We gratefully acknowledge the NNSF of China (21275119, 51473136 and 21575116).

Appendix A. Supplementary material

Supplementary data associated with this article can be found in the online version at http://dx.doi.org/10.1016/j.bios.2016.08.032.

References

Astruc, D., Boisselier, E., Ornelas, C., 2010. Chem. Rev. 110, 1857–1959.
Carmi, N., Breaker, R.R., 2001. Bioorg. Med. Chem 9, 2589–2600.
Carmi, N., Balkhi, S.R., Breaker, R.R., 1998. Proc. Natl. Acad. Sci. USA 95, 2233–2237.
Chen, J.H., Zhou, X.M., Zeng, L.W., 2013. Chem. Commun. 49, 984–986.
Cuenoud, B., Szostak, J.W., 1995. Nature 375, 611–614.
Cui, L., Wu, J., Li, J., Ju, H.X., 2015. Anal. Chem. 87, 10635–10641.
Gao, C., Yu, X.Y., Xu, R.X., Liu, J.H., Huang, X.J., 2012. ACS Appl. Mater. Inter 4; , pp. 4672–4682.
Gao, X.H., Du, C., Zhuang, Z.H., Chen, W., 2016. Chem. Commun. . http://dx.doi.org/10.1039/c6tc02055k
Gao, X.H., Lu, Y.Z., He, S.J., Li, X.K., Chen, W., 2015b. Anal. Chim. Acta 879, 118–125.
Gao, X.H., Lu, Y.Z., Zhang, R.Z., He, S.J., Ju, J., Liu, M.M., Lia, L., Chen, W., 2015a. J. Mater. Chem. C 3, 2302–2309.
Groves, J.T., 2000. J. Porphy. Phtha 4, 350–352.
He, H.L., Xu, X.L., Wu, H.X., Jin, Y.D., 2012. Adv. Mater. 24, 1736–1740.
Huang, Y.S., Ma, Y.L., Chen, Y.H., Wu, X.M., Fang, L.T., Zhu, Z., Yang, C.Y.J., 2014. Anal. Chem. 86, 11434–11439.
Hun, X., Xie, G.L., Luo, X.L., 2015. Chem. Commun. 51, 7100–7103.
Jiang, Y., Li, B.L., Milligan, J.N., Bhadra, S., Ellington, A.D., 2013. J. Am. Chem. Soc. 135, 7430–7433.
Ju, J., Chen, W., 2014. Biosens. Bioelectron. 58, 219–225.
Li, B., Ellington, A.D., Chen, X., 2011. Nucleic Acids Res. 39, e110.
Li, F., Yang, L.M., Chen, M.Q., Qian, Y., Tang, B., 2013. Biosens. Bioelectron. 41, 903–906.
Li, J., Lu, Y., 2000b. J. Am. Chem. Soc. 122, 10466–10467.
Li, J., Zheng, W., Kwon, A.H., Lu, Y., 2000a. Nucleic Acids Res. 28, 481–488.
Lim, B., Xia, Y.N., 2011. Angew. Chem. Int. Ed. 50, 76–85.
Liu, G.P., Wu, Y.M., Yuan, Y.L., Chai, Y.Q., Wei, S.Q., Zhang, D.J., 2014. RSC Adv. 4, 52117–52122.
Liu, J., Cao, Z., Lu, Y., 2009. Chem. Rev. 109, 1948–1998.
Liu, J., Brown, A.K., Meng, X., Cropek, D.M., Istok, J.D., Watson, D.B., Lu, Y., 2007. Proc. Natl. Acad. Sci. USA 104, 2056–2061.
Liu, S.F., Cheng, C.B., Gong, H.W., Wang, L., 2015. Chem. Commun. 51, 7364–7367.
Meng, H.M., Zhang, X.B., Lv, Y.F., Zhao, Z.L., Wang, N.N., Fu, T., Fan, H.H., Liang, H., Qiu, L.P., Zhu, G.Z., Tan, W.H., 2014. ACS Nano 8, 6171–6181.
Nitta, Y., Kuroda, R., 2006. Biopolymers 81, 376–391.
Pasternack, R.F., Gibbs, E.J., Villafranca, J.J., 1983. Biochemistry 22, 2406–2414.
Santoro, S.W., Joyce, G.F., 1997. Natl. Acad. Sci. USA 94, 4262–4266.
Sobin, C., Parisi, N., Schaub, T., Gutierrez, M., Ortega, A.X., 2011. Arch. Environ. Contam. Toxicol. 61, 521–529.
Sun, Y.H., Kong, R.M., Lu, D.Q., Zhang, X.B., Meng, H.M., Tan, W.H., Shen, G.L., Yu, R. Q., 2011. Chem. Commun. 47, 3840–3842.
Tang, S.R., Tong, P., Li, H., Tang, J., Zhang, L., 2013. Biosens. Bioelectron. 42, 608–611.
Tao, C.Y., Yan, Y.R., Xiang, H., Zhu, D., Cheng, W., Ju, H.X., Ding, S.J., 2015. Chem. Commun. 51, 4220–4222.
Wu, H., Liu, Y.L., Wang, H.Y., Wu, J., Zhu, F.F., Zou, P., 2016. Biosens. Bioelectron. 81, 303–308.
Xie, S.B., Chai, Y.Q., Yuan, Y.L., Yuan, R., 2014. Chem. Commun. 50, 7169–7172.
Xu, J., Wu, J., Zong, C., Ju, H.X., Yan, F., 2013. Anal. Chem. 85, 3374–3379.
Xu, J.J., Zhao, W.W., Song, S.P., Fan, C.H., Chen, H.Y., 2014. Chem. Soc. Rev. 43, 1601–1611.
Yin, B.C., Ye, B.C., Tan, W.H., Wang, H., Xie, C.C., 2009a. J. Am. Chem. Soc. 131, 14624–14625.
Yin, B.C., Ye, B.C., Tan, W.H., Wang, H., Xie, C.C., 2009b. J. Am. Chem. Soc. 131, 14624–14625.
Yin, P., Choi, H.M., Calvert, C.R., Pierce, N.A., 2008. Nature 451, 318–322.
Zhang, H., Jin, M.S., Liu, H.Y., Wang, J.G., Kim, M.J., Yang, D., Xie, Z.X., Liu, J.Y., Xia, Y. N., 2011. ACS Nano 10, 8212–8222.
Zhang, J., Yuan, Y.L., Xie, S.B., Chai, Y.Q., Yuan, R., 2014b. Biosens. Bioelectron. 60, 224–230.
Zhang, R.Z., Chen, W., 2014a. Biosens. Bioelectron. 55, 83–90.
Zhang, Y., Zeng, G.G., Tang, L., Chen, J., Zhu, Y., He, X.X., He, Y., 2015a. Anal. Chem. 87, 989–996.
Zhang, Y., Yan, Y.R., Chen, W.H., Cheng, W., Li, S.Q., Ding, X.J., Li, D.D., Wang, H., Ju, H. X., Ding, S.J., 2015b. Biosens. Bioelectron. 68, 343–349.
Zheng, Y.N., Yuan, Y.L., Chai, Y.Q., Yuan, R., 2016. Biosens. Bioelectron. 79, 86–91.